Original scientific article
http://dx.doi.org/10.59456/afts.2024.1630.079M

LIQUEFACTION-INDUCED DAMAGE IN THE CITIES OF ISKENDERUN AND GOLBASI AFTER THE 2023 TURKEY EARTHQUAKE

Milev Nikolay[1], Takashi Kiyota[2], Briones Juan[3], Briones Othon[3], Cinicioglu Ozer[5], Torisu Seda[6]

[1]*University of Architecture, Civil Engineering and Geodesy (UACEG), Department of Geotechnics, Sofia, Bulgaria, e-mail: milev_fte@uacg.bg*
[2]*The University of Tokyo, Institute of Industrial Science, Tokyo, Japan*
[3]*Geofizika EIG Ltd., Plovdiv, Bulgaria*
[5]*Department of Civil Engineering, Bogazici University, Istanbul, Turkey*
[6]*Nuclear Facilities Division, Obayashi Corporation, Tokyo, Japan*

SUMMARY

On February 6th 2023 two major earthquakes struck southeast Turkey, M7.7 Kahramanmaras and M7.6 Elbistan, respectively. Unfortunately, due to the impact of these catastrophic events more than 50 000 casualties and 35 000 collapsed buildings have been reported since then. The aim of the study is to demonstrate preliminary site response analysis and assessment of re-liquefaction potential of sites which have been affected by the earthquakes – especially the cities of Iskenderun and Golbasi. Both site-specific areas have clear evidences of liquefaction and lateral spreading events which imply the focus of the presented paper. A series of geophysical MASW and microtremor tests have been performed in order to determine shear wave velocities up to depth of 30 m as well as the fundamental natural frequency of the soil deposits.

Moreover, samples have been collected from sand and silt ejecta in order to evaluate some basic physical properties – grain-size curves, specific gravity and plasticity parameters. On the basis of the obtained data seismic classification of the investigated sites according to current design codes has been made and in-depth distance to relatively stiff layer has been assumed. For the sake of evaluating risk of re-liquefaction the widely-used simplified stress-based approach to triggering assessment has been adopted considering some rules of the thumb (e.g., sieve analysis and plasticity properties evaluation). Lastly, post-liquefaction reconsolidation settlement and lateral displacement have been determined in terms of future earthquakes.

Key words: *lateral spreading, liquefaction assessment, shear wave velocity, microtremor, microseismic characterization, Iskenderun, Golbasi, 2023 Turkey-Syria Earthquake*

INTRODUCTION

Following the significant seismic events that transpired in Turkey and Syria on February 6th, 2023, a joint reconnaissance team was swiftly assembled. This multidisciplinary team brought together researchers and engineers hailing from Japan, Turkey, and Bulgaria, representing prominent organizations in the field of earthquake engineering. These organizations included the Japan Association for Earthquake Engineering, the Architectural Institute of Japan, the Japan Society of Civil Engineers, the Japanese Geotechnical Society, Bogazici University, MEF University, and the

University of Architecture, Civil Engineering and Geodesy (UACEG). Their collaborative efforts culminated in an extensive on-site investigation conducted between March 28th and April 2nd, 2023, which transpired approximately two months after the catastrophic earthquakes.

During the survey of the Islahiye region, several noteworthy findings came to light. Among them, a landslide event had transpired, leading to the formation of a landslide dam. Furthermore, another landslide occurrence unfolded in Tepehan, impacting a relatively gentle slope predominantly composed of limestone. This event sparked inquiries regarding potential links to fault movements.

The city of Iskenderun encountered a multifaceted array of challenges in the aftermath of the seismic events. In addition to documented building collapses occurring on soft ground, instances of building tilting and ground subsidence were attributed to the liquefaction of reclaimed coastal soil. These complexities further compounded the post-earthquake scenario.

In Golbasi, the survey revealed significant structural damage in buildings with shallow foundations that were situated on soft ground. This damage was primarily attributed to liquefaction-induced effects, including tilting and settlement. However, a more detailed investigation is imperative to precisely delineate the extent of liquefied soil layers in the area.

Antakya and Kahramanmaras emerged as regions where building damage correlated with surface ground vibrations. Despite experiencing severe building collapses, Antakya exhibited relatively stable ground conditions characterized by an average shear wave velocity (V_s) exceeding 400 m/s. This suggests the possibility of wave amplification linked to underlying geological factors. Conversely, Kahramanmaras witnessed notable building damage concentrated in alluvial fan formations.

This collaborative reconnaissance mission has yielded invaluable insights into the diverse impacts of the earthquakes on different regions – survey route is presented on Figure 1. It underscores the critical importance of conducting further research and comprehensive investigations to gain a complete understanding of the underlying geological and geotechnical factors contributing to these effects. Such knowledge will be instrumental in enhancing earthquake preparedness and mitigation measures in these areas.

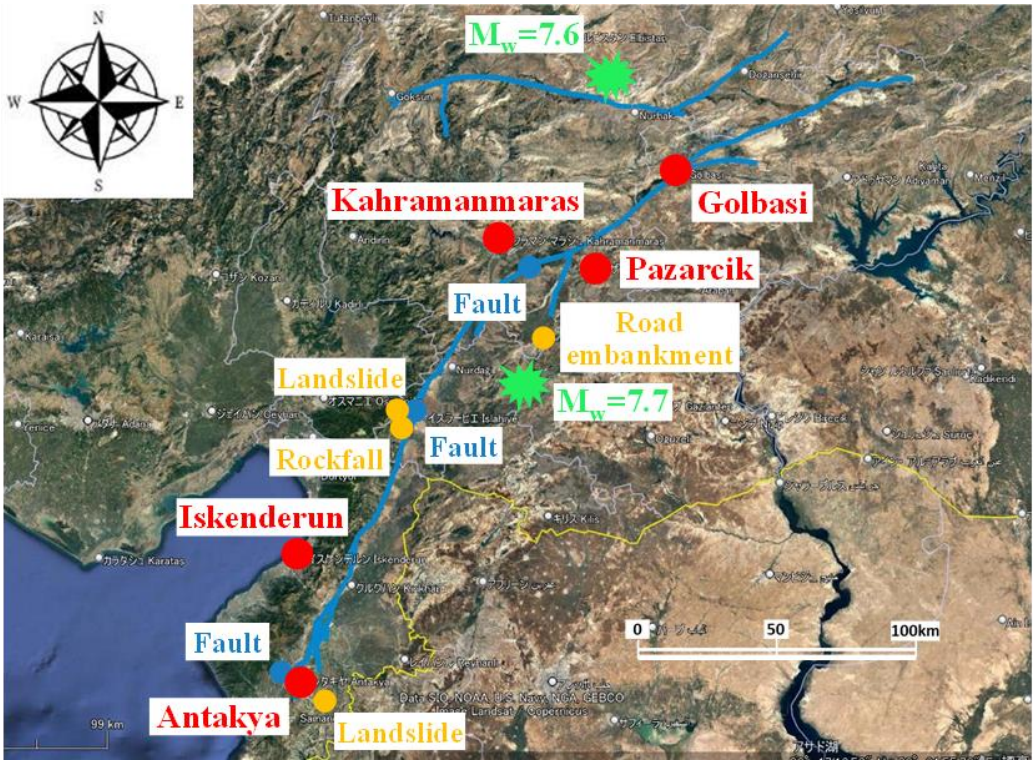

Figure 1. Map of the affected area (including fault and epicenter) – survey route

EARTHQUAKE CHARACTERISTICS

On February 6th, 2023, at 4:17 local time (1:17 GMT), a significant earthquake, measuring 7.7 on the moment magnitude (M_w) scale, with a focal depth of 8.6 km, struck in the vicinity of Kahramanmaras (epicenter: 37.228N, 37.043E) along the East Anatolian Fault, which traverses the border between Turkey and Syria. Roughly nine hours later, at 13:24 local time (10:24 GMT), another major earthquake, with a moment magnitude (M_w) of 7.6 and a focal depth of 7.0 km, occurred in Elbistan (epicenter: 38.089N, 37.239E) in the same region. Subsequently, on February 20th, the region experienced a significant aftershock, registering a moment magnitude (M_w) of 6.4 with a focal depth of 22 km, centered in Hatay (epicenter: 36.037N, 36.021E). These seismic events resulted in devastating consequences, including a significant loss of life, widespread destruction of more than half a million structures, including critical infrastructure such as communication and energy facilities, and substantial economic losses [1].

These earthquakes induced left-lateral fault ruptures along the East Anatolian Fault, spanning from Malatya to Hatay and covering a distance of approximately 320 km. While the severe damage to buildings and pipelines along this rupture has been discussed elsewhere in the context of lifeline impacts, this study primarily focuses on the geotechnical damage arising from the intense ground shaking. The most intense recorded ground motion was observed at the Pazarcik station [2]. The earthquake's duration was approximately 60 seconds, during which peak horizontal ground accelerations exceeded 2*g* (where *g* represents the acceleration due to gravity, approximately 9.81 m/s²). Notably, this earthquake generated numerous strong-motion records collected by seismographs located in close proximity to the fault, which spans over 300 km in length [2]. These records not only help address gaps in the existing attenuation equation for short distances from the hypocenter but also provide valuable insights into the generation mechanism of ground motion associated with fault movement. The maximum acceleration recorded near the epicenter significantly surpassed the predictions of previous attenuation equations.

In response to this catastrophic event, a collaborative reconnaissance team was assembled, comprising researchers and engineers from Japan, Turkey, and Bulgaria. This team was organized by prominent earthquake engineering organizations, including the Japan Association for Earthquake Engineering (JAEE), the Architectural Institute of Japan (AIJ), the Japan Society of Civil Engineers (JSCE), the Japanese Geotechnical Society (JGS), Bogazici University, MEF University, and the University of Architecture, Civil Engineering and Geodesy (UACEG). Led by Professor Kusunoki of the Institute of Industrial Science, University of Tokyo, this team conducted an extensive on-site investigation from March 28th to April 2nd, 2023, approximately two months after the earthquakes. The team consisted of 27 Japanese members, 22 Turkish professors and practitioners, 1 Bulgarian researcher and 2 Mexican geophysicists and with their base of operations in Gaziantep. They conducted daily visits to different disaster-affected areas for assessments.

As mentioned earlier, these earthquakes led to widespread destruction of buildings and a significant loss of life. One of the main objectives of the geotechnical field investigation was to determine whether the extent of such damage depended not only on the structural characteristics of buildings but also on the seismic properties of the soil. Due to time constraints, the decision was made to focus the survey on sites and towns with pre-existing information available. In addition to ground-based assessments, aerial surveys using drones were conducted to evaluate damage over a broader area. Various geotechnical investigation methods were utilized, including the portable dynamic cone penetration test (PDCPT), the multichannel analysis of surface wave (MASW), and microtremor-based horizontal-to-vertical spectral ratio (H/V) measurements, to characterize ground properties. Furthermore, interviews were conducted with local residents.

For the sake of converting portable dynamic cone penetration test (PDCPT) blow counts (N_d) to NSPT (standard penetration test, SPT, values), an equation proposed by [3], was employed, assuming sandy soil characteristics:

$$N_{SPT} = 0.66_x N_d \text{ (when } N_d \leq 4) \text{ and } N_{SPT} = 1.1 + 0.30_x N_d \text{ (when } N_d > 4) \quad (1)$$

The study area is situated in the southeastern part of Turkey, extending from Kahramanmaras to Antakya. This region is surrounded by elevated mountain ranges on all sides, including the Amanos Mountains to the west (comprising pre-Cambrian to Eocene rock units), the Southeast Anatolian Mountain Range to the east (comprising Cretaceous to Miocene rock units), and the Baer-Bassit Range to the south (predominantly composed of Cretaceous ophiolite and Miocene rock units). The region features diverse topography, including multiple mountain ranges, river valleys, and plateaus. It is located at the convergence of the Arabian and African tectonic plates with the Anatolian block, making it seismically active and contributing to its varied topography. Key fault zones in this region include the East Anatolian Fault Zone (EAFZ), Dead Sea Fault Zone (DSFZ), and Karasu Fault System (KFS). Several residential areas are located within Quaternary geological units in the graben, primarily consisting of alluvial fans, alluvium, and basaltic compound volcanic rocks.

ISKENDERUN CITY

The city of Iskenderun, located on the Mediterranean coast with a population of approximately 500 000 residents, is situated approximately 100 kilometers away from the earthquake's epicenter and approximately 15 kilometers west of the earthquake fault. Iskenderun experienced relatively minimal structural damage compared to Kahramanmaras and Antakya. However, it did suffer significant damage due to geotechnical issues, primarily in areas with land reclamation. Unfortunately, there are no available strong motion records for Iskenderun.

Figure 2 displays a map of Iskenderun, where a survey was conducted on March 31st. The ground in Iskenderun predominantly consists of Quaternary alluvium containing silt and sandy layers, as observed in the Konarli area of Iskenderun Bay. This region has loose soil and a high water table [4]. Iskenderun, once a small town surrounded by marshland, underwent substantial development between the mid-19th century during the Ottoman Empire and the French Mandate period, lasting until the first half of the 20th century. Figure 2 illustrates the location of the lighthouse, which was originally at sea, and the coastal area beyond this point has been transformed into modern reclaimed land. After the earthquake on February 6th [5], it was reported that streets near the coast were inundated by seawater. During the authors' survey on March 31st, inundation was confirmed due to rainfall the previous day. Figure 2 also displays the inundated area during the survey, primarily in the reclaimed land area, with the coastal shopping street submerged by about 30 centimeters. Moreover, in the eastern part of the survey area, the inundation extended further inland. Local residents indicated that this area was once marshland, possibly resulting in more pronounced subsidence on the elevated ground in the eastern part. Numerous signs of sand ejecta were also observed in and around the inundated region.

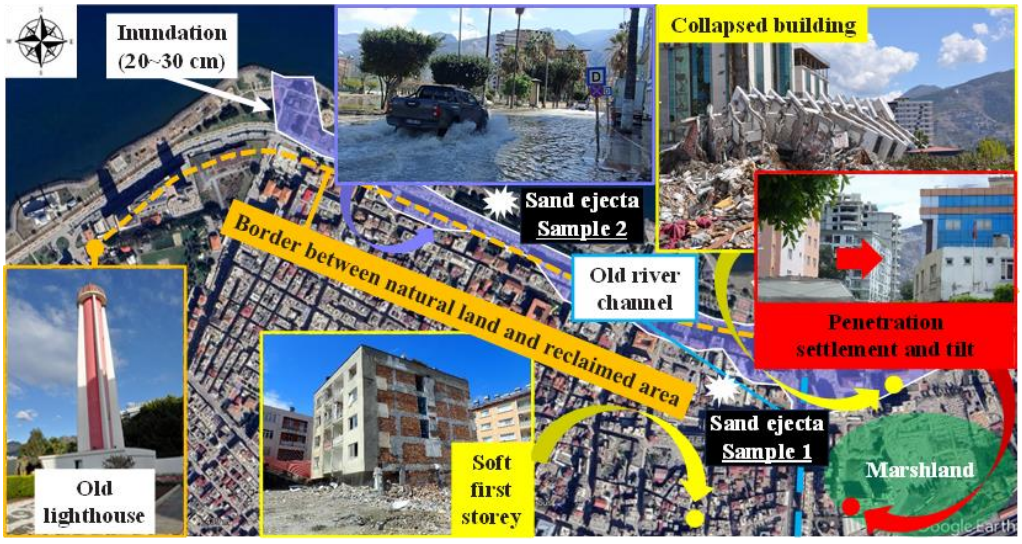

Figure 2. Reclaimed land boundary and inundation area in Iskenderun City observed in the authors' survey on 31st March, 2023

Figure 2 additionally illustrates damage caused by liquefaction, including slight building subsidence and significant sidewalk uplift. This street was previously a water channel [6], potentially making the reclaimed soil in the channel susceptible to liquefaction during the earthquake. Figure 3 and Figure 4 depict typical structural damage in Iskenderun. Figure 3 shows a mid-rise building in reclaimed land, where the entire structure has tilted significantly.

Figure 3. Evidence of various kinds of geotechnical problems observed in Iskenderun

Figure 4. Collapsed building located in the former marshland – near Hotel Ramada

Similar damage, characterized by tilting and settlement of buildings, is evident along coastal streets, albeit to varying degrees (Fig. 5 and Fig. 6). This damage is likely attributed to liquefaction of the reclaimed ground and loss of bearing capacity. In contrast, the structure shown in Figure 4, located in an area formerly marshland, collapsed in a twisting manner. Information on the distribution of structural damage patterns in Iskenderun City is currently limited, but it is observed that there was relatively more structural damage due to seismic motion inland from the reclamation boundary. Both geotechnical issues and structural damage occurred in the marshland area. Different surface ground

characteristics and the presence or absence of liquefaction likely contributed to distinct patterns of structural damage.

Figure 5. Tilted middle-rise buildings near the sea-coast (at the beginning of the reclaimed land)

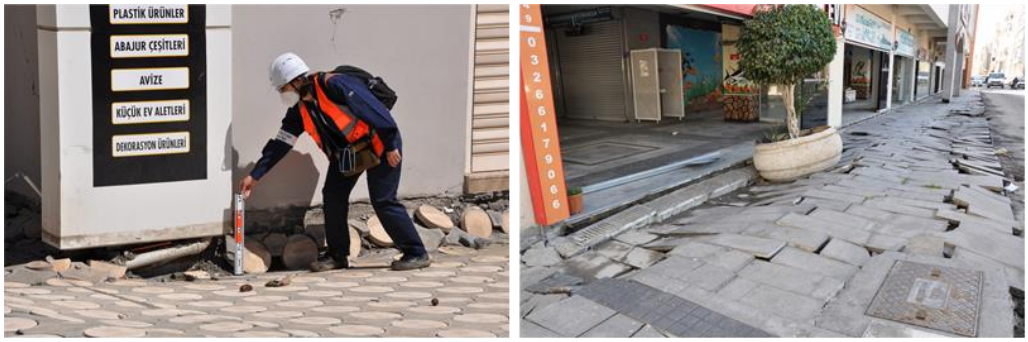

Figure 6. Settlement of buildings due to soil liquefaction

Figure 8 illustrates the reclaimed area where the promenade along the seashore subsided significantly, by approximately 50 centimeters, nearly aligning with the sea level. This subsidence likely led to the inundation of coastal streets by high waves. Observations also noted water flowing backward and emerging from sewage manholes on the inundated coastal street. The blockage of sewage pipelines due to liquefied soil deformation likely caused extensive inundation damage.

Figure 7. Location of performed tests in the city of Iskenderun (36°35'33.99"N, 36°10'6.98"E)

Figure 7 presents the exact location and Figure 11 results of the PDCPT at DP-3 and the multichannel analysis of surface wave (MASW) at SW-1. The PDCPT was conducted down to a depth of ground level -4.0 meters, revealing that the groundwater table was almost at the surface. The N_{SPT} values at the top surface were consistently low, less than 5, and slightly increased, ranging from 5 to 10, from ground level -1.0 meter to -2.0 meters. Below this depth, the soil layer exhibited loose characteristics, with N_{SPT} values averaging around 5. As shown in Figure 8, several cracks, each several tens of

centimeters wide, were identified in the reclaimed land due to lateral spreading, and numerous sand ejecta were observed, indicating that coastal area land subsidence was induced by liquefaction. Calculating the distance of cracks from the seashore to be 60 meters inland, the lateral displacement was estimated to be as much as 1.5 meters toward the sea.

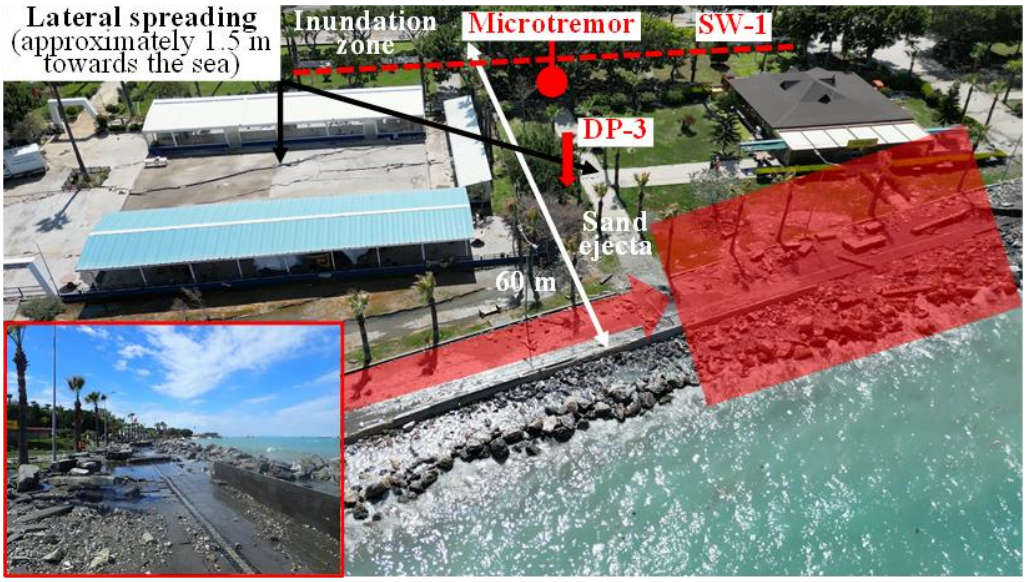

Figure 8. Liquefaction-induced damages in the reclaimed land (36°35'33.99"N, 36°10'6.98"E)

The shear wave velocity value of the surface layer from the MASW was consistently less than 150 m/s but gradually increased up to approximately ground level -10 meters, reaching about 190 m/s (Fig. 10). At greater depths, the shear wave velocity value remained relatively stable until about ground level - 25 meters. Given these findings, it can be reasonably concluded that the observed 50 cm subsidence along the shoreline was a result of liquefaction in the reclaimed ground up to approximately ground level -10 meters, especially considering the occurrence of lateral spreading. However, it should be noted that the inundation damage in Iskenderun City was more severe immediately after the earthquake. Further investigations are necessary to explore the causes of land subsidence in the city, which may not solely be attributed to liquefaction but also to crustal deformation effects.

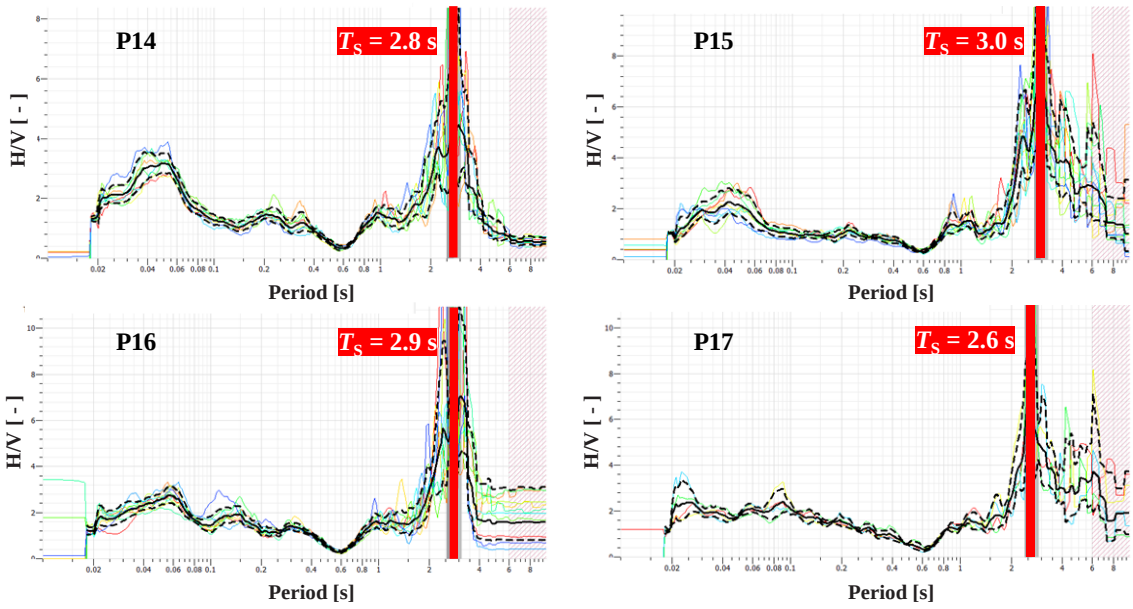

Figure 9. Results from microtremor tests – evaluation of predominant period of the soil profile at P14, P15, P16 and P17

During this survey, two distinct soil samples, referred to as Sample 1 and Sample 2, were collected, with their specific locations illustrated in Figure 2. Both samples, identified as sand ejecta, exhibit a specific gravity of 2.68. Notably, the particle distribution curves for these samples are remarkably similar, characterizing them as poorly graded and "highly liquefiable" soils. Moreover, a thorough evaluation of site-specific soil characteristics to advance our understanding of seismic site response was conducted. Cutting-edge geophysical techniques for direct measurements of key parameters were utilized. The MASW method was employed to determine the shear wave velocity (V_{s30}), representing the average shear wave velocity in the upper 30 meters of the soil medium at the study site. Additionally, the microtremor-based horizontal-to-vertical spectral ratio (H/V) method was employed in order to derive the predominant period of the soil profile (T_s), resulting in an average T_s value of 2.8 seconds (Fig. 9). These measurements provided critical input parameters for further seismic hazard analysis. Based on this data, the average depth (H) to a stiff layer with a shear-wave velocity greater than 800 m/s within the soil profile was estimated using the classic formula $H = (4 \text{ x } V_{s30}) / T_s$ [7], resulting in an estimated H value of approximately 130 meters. These findings offer valuable insights into site-specific seismic response characteristics, crucial for seismic hazard assessment and infrastructure design in the studied region. According to Eurocode 8, the classification of a soil profile based on its shear wave velocity in the upper 30 meters (V_{s30}) is a fundamental step in assessing seismic hazard. When V_{s30} falls into the Type D category, it indicates that the soil profile consists of relatively soft and potentially liquefiable soils. This classification holds significant implications for seismic risk assessment and structural design since Type D soil profiles are associated with increased ground motion amplification and heightened seismic vulnerability.

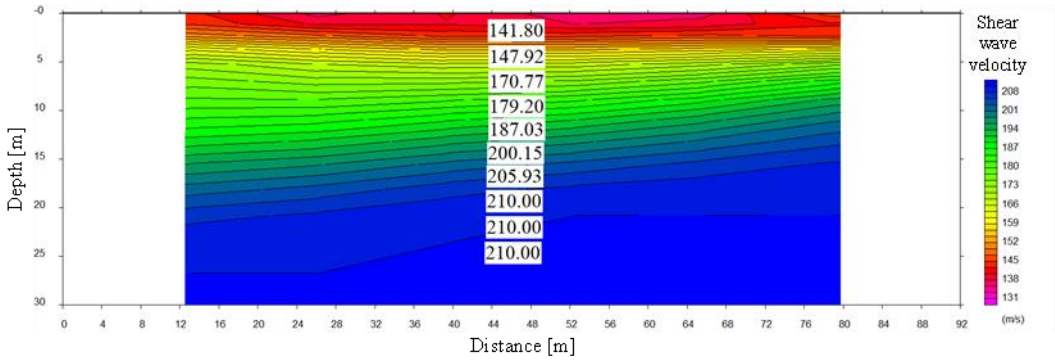

Figure 10. 2D shear wave velocity profile based on MASW measurements at SW-1

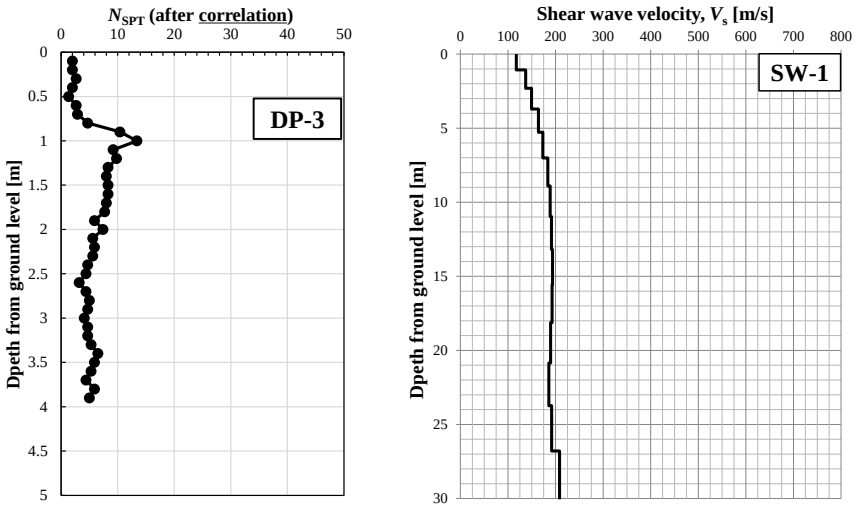

Figure 11. Results of PDCPT at DP-3 and MASW at SW-1

Liquefaction assessment within this study adhered to a robust deterministic framework, combining crucial data from two primary sources: 1) results obtained through PDCPT, converted to N_{SPT} [8,9, 10], and 2) shear wave velocity (V_s) profile [11,12]). The calculated factor of safety (FS) consistently revealed values below unity, indicating the susceptibility of the soil profile to liquefaction-induced

phenomena. This susceptibility necessitated a meticulous examination of potential consequences, encompassing liquefaction-induced reconsolidation settlement and lateral spreading phenomena [13,14,15,16,17,18,19]. The results, as presented in Figure 13, portray a conservative outlook on the liquefaction potential. However, it is imperative to exercise discernment in interpreting these findings. Some layers within the soil profile may exhibit relatively low V_s values, potentially raising concerns regarding their liquefaction susceptibility. Nonetheless, a profound understanding of the physical properties (especially particle size distribution curve and plasticity parameters) of these specific layers might mitigate these concerns. Their intrinsic characteristics, such as high confining pressures, significant fines content, or cementation, effectively preclude them from active participation in the liquefaction response. Thus, the comprehensive liquefaction assessment underscores the importance of considering not only the quantitative data but also the qualitative aspects of soil behavior, ensuring a holistic understanding of site-specific seismic risk. Such knowledge is invaluable for seismic hazard assessment and resilient infrastructure design in the region.

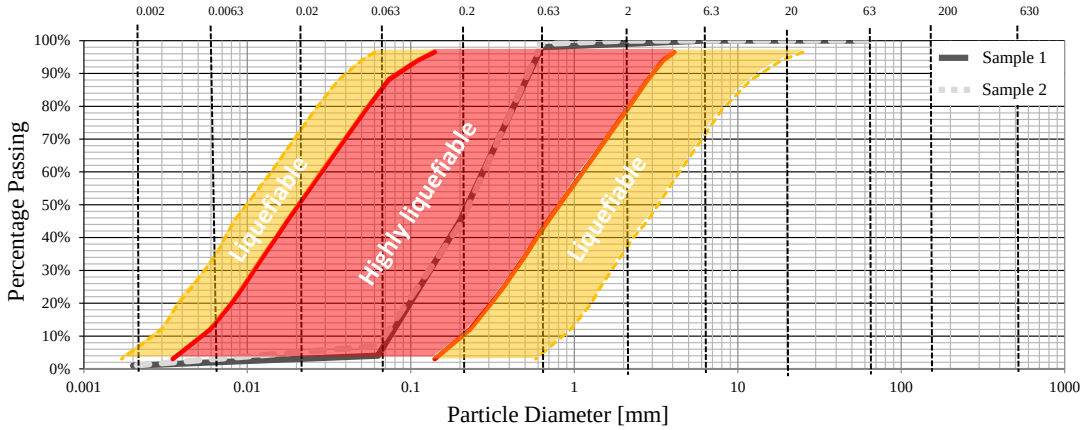

Figure 13. Particle distribution curves of sand ejecta (Sample 1 and Sample 2) collected from the city of Iskenderun – comparison with critical range associated with liquefaction

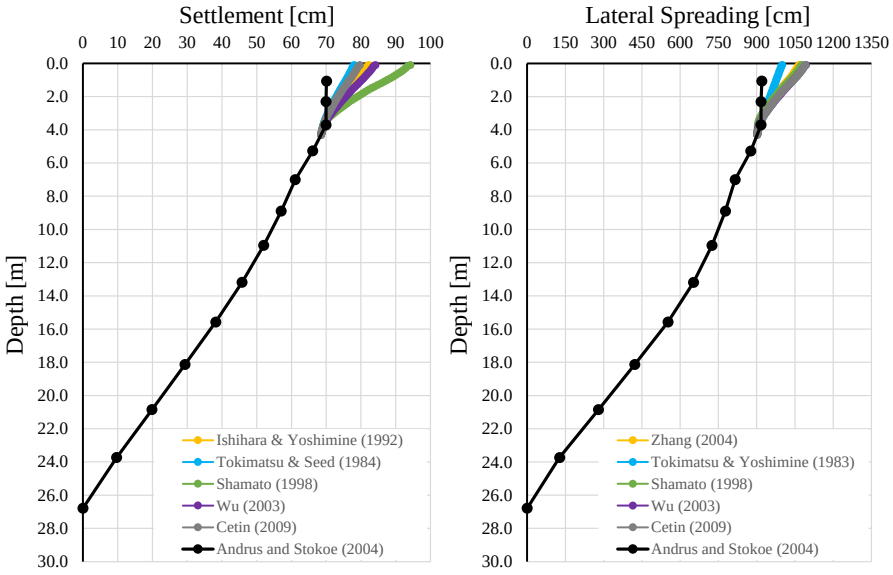

Figure 13. Evaluation of settlement and lateral spreading due to possible re-liquefaction in the city of Iskenderun by simplified procedures

GOLBASI TOWN

The Golbasi Basin is characterized as a pull-apart basin with a left-lateral strike-slip fault along the Golbasi-Turkoglu segment, situated on the East Anatolian Fault Zone (EAFZ). Golbasi Lake in this region resembles a sag pond. A study conducted by [20] revealed that the lithological units in the

examined area primarily consist of Quaternary alluvial deposits (Qal), including clay, silt, sand, and gravel, along with swamp sediments (Qb). In terms of groundwater levels, they typically range from -0.65 meters to -3.5 meters, except in three boreholes where no water was detected. The dominant ground vibration period varies from 0.23 to 0.67 seconds, averaging at 0.48 seconds. As a result of this investigation, the region has been designated as a priority area for preventive measures. It has been categorized into two zones: OA1, where Qal formation prevails, primarily addressing earthquake hazards, and OA2, where Qb formation is dominant, focusing on mass movement hazards and high slopes.

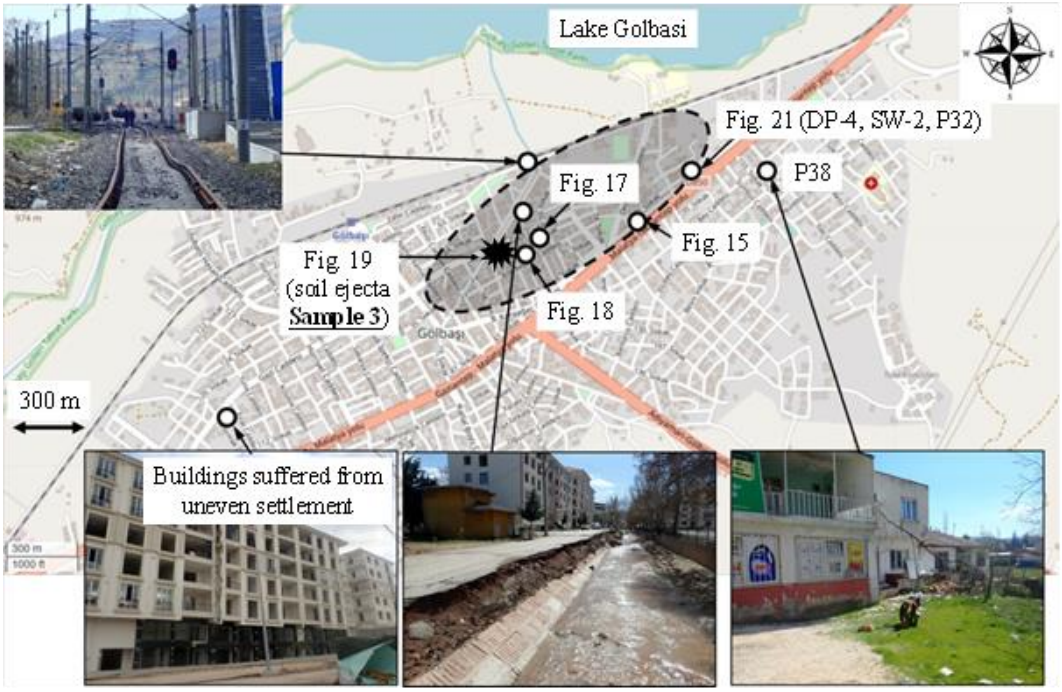

Figure 14. Extent of the liquefaction-induced damages in the town of Golbasi

Figures 16, 17, 18 and 19 depict typical building damages. Figure 16 shows the most severely tilted building identified during the authors' survey, leaning against an adjacent structure. The groundwater level at the foundation of this building, which exhibited pronounced tilting, was approximately at ground level -1.0 meter.

Figure 15. Tilted foundation of demolished building [5]

Golbasi, a town with around 35 000 residents situated approximately 85 kilometers northeast of the earthquake epicenter, experienced damage due to liquefaction. This led to settlement and tilting issues in many mid-rise buildings. The damage was particularly severe in the southern part of Golbasi, adjacent to Lake Golbasi. This substantial damage was attributed to loose lake sediments and the prevalence of shallow foundations in most buildings. For instance, Figure 15 illustrates the foundation of a five-story building, which initially had a 3-meter-deep foundation but was completely overturned by the earthquake by the time of the authors' survey on April 1st. The remaining mat foundation measured approximately 0.8 meters in thickness. It is likely that many mid-rise buildings in Golbasi had similar shallow foundation types. Numerous structures in this area suffered from settlement and tilting damage due to insufficient bearing capacity of the soil, especially along the demarcated area near the lake on the main road (D360), as depicted in Figure 14. This region also witnessed damage to the water channel's retaining wall and subsidence of the railway track.

Aerial imagery in Figure 16, captured from a northwest perspective, reveals significant subsidence and tilting damage affecting nearly all mid-rise buildings within the frame. Figure 17 features a building that experienced extensive settlement, subsiding by approximately 1.5 meters, causing cars to become wedged into the parking space's ceiling. Additionally, Figure 18 showcases notable settlement of mid-rise buildings on both sides of a narrow road, accompanied by substantial uplift of the road surface. These damages correspond to significant ground deformations, with minimal structural damage to walls and columns. However, Figure 19 illustrates a severely damaged building where the ground floor's walls and columns failed due to seismic motion, subsequently sinking into the soil. According to interviews with local residents, one building (green and white) reputedly had a pile foundation and incurred substantial settlement and tilting damage, as illustrated in Figure 19. Specifics regarding this building's pile foundation remain unclear at present.

Figure 20 and Figure 21 display the locations and Figure 23 demonstrates the results of PDCPT (PD-4) and MASW (SW-2) assessments conducted near a heavily subsided and tilted building. The N_{SPT} values were exceptionally low, registering less than 5 up to ground level -3.0 meters and gradually increasing beyond that depth. Conversely, the shear wave velocity values exhibited minimal values of 130-140 m/s up to ground level - 7.0 meters, followed by a slight increase with depth. Loose soils extended continuously down to ground level - 20 to - 25 meters. These findings suggest that the shallow surface soil layer, characterized by liquefaction and loss of bearing capacity, led to considerable settlement and tilting in structures. Borehole data from the city of Golbasi has been analyzed [20], revealing that the lake-side region adjacent to the main road (D360) predominantly comprised soft clay. Nevertheless, same study also identifies pockets of medium-dense sand and gravelly soils, which align relatively closely with the area demarcated by the broken line in Figure 14. This implies that significant liquefaction may have occurred in these medium-dense sand or gravelly soil sections.

Figure 16. Heavily tilted building and surrounding buildings with similar damage

Figure 17. Building suffered from subsidence of about 1.5 m – before and after the earthquake

Figure 18. Road uplift and settlement / tilting damage to buildings on either side of the road

19. Structural damage (soft first storey) – blue building, and settlement / tilting damage of a building (green and white) that reportedly had pile foundations

Furthermore, the ejected soil collected near the green and white building in Figure 19 primarily consisted of reddish-colored silt and clay, characterized by a substantial plasticity index (*PI*) of 20. According to liquefaction assessment standards established by JRA and AIJ (REF), soils with a

plasticity index exceeding 15 are deemed unlikely to liquefy and are thus exempt from liquefaction analysis. This suggests that liquefaction may have taken place at the source of the ejected clayey soil, or alternatively, the surface clayey soil could have been entrained in the ejected water resulting from liquefaction in the underlying sand or gravelly soil layers, subsequently surfacing.

Figure 20. Location of performed tests in the town of Golbasi (37°47'26.57"N, 37°39'7.88"E)

While this survey included PDCPT and MASW evaluations conducted immediately adjacent to the main road, confirming the thickness of the soft surface layer, it is conceivable that the thickness of the soft layer may increase closer to the lake. Additionally, subsidence and tilting damage to buildings resulting from ground deformation were observed on the western boundary of Golbasi, as indicated on the map in Figure 14. Consequently, further investigations are imperative to ascertain the liquefied soil layer and its distribution in the future. Figure 24 illustrates particle size distributions for soils typically associated with liquefaction, and the envelope of soil considered susceptible to liquefaction [21]. Samples from soil ejecta were collected right next to green and white building on Figure 19, and particle size tests were conducted in the laboratory. The resulting particle size distribution curve was then compared to the particle size distributions for soils typically associated with liquefaction. It is evident that a significant portion of the curve falls within the "highly liquefiable" region. Moreover, the evaluation of liquefaction susceptibility incorporates three established procedures: those proposed by [22,23] and the criteria outlined in the Japanese Road Bridge Design Standards. These methods are based on analyzing fundamental physical soil properties, including the Plastic Index (*PI*), Liquid Limit (LL), and Fines Content (*FC*). According to these simplified assessment techniques, the soil in the Golbasi region is classified as "moderately susceptible to liquefaction" – Figure. 25 and Figure. 26. This categorization is critical, emphasizing the need for vigilance, especially given the severe damages in Golbasi associated with such soil classifications.

Figure 21. Locations of PDCPT, MASW and microtremor measurement conducted near buildings with subsidence / tilting damage (37°47'26.57"N, 37°39'7.88"E)

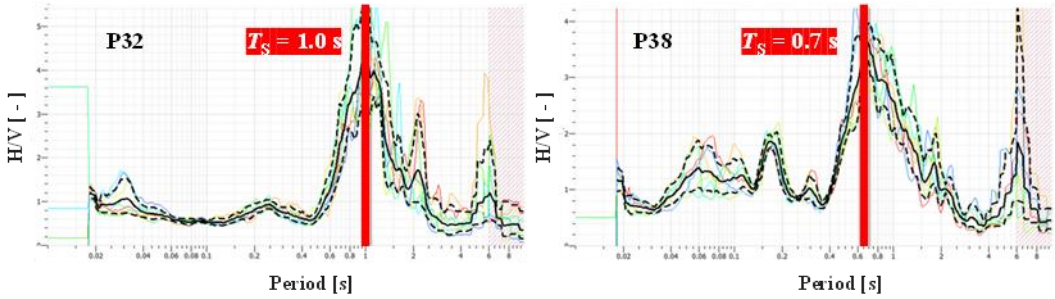

Figure 22. Results from microtremor tests – evaluation of predominant period of the soil profile at P32 and P38

In parallel measurements conducted in the city of Iskenderun, a similar suite of tests to assess site-specific soil characteristics was employed. The shear wave velocity (V_{s30}) in Golbasi was determined to be approximately 170 m/s, and the predominant period of the soil profile (T_s) was measured at 1.0 second, with a specific focus on point P32, a location associated with numerous liquefaction occurrences (Figure 22). The estimated depth (H) to a stiff layer with a shear-wave velocity exceeding 800 m/s within the soil profile was found to be around 43 meters. The outcome of this evaluation led to the categorization of the soil as Type D in the context of Eurocode 8, indicating the existence of relatively soft and potentially liquefiable soils. This classification holds notable consequences for seismic risk assessment and structural design, primarily due to the elevated levels of ground motion amplification and heightened seismic vulnerability typically associated with Type D soil profiles.

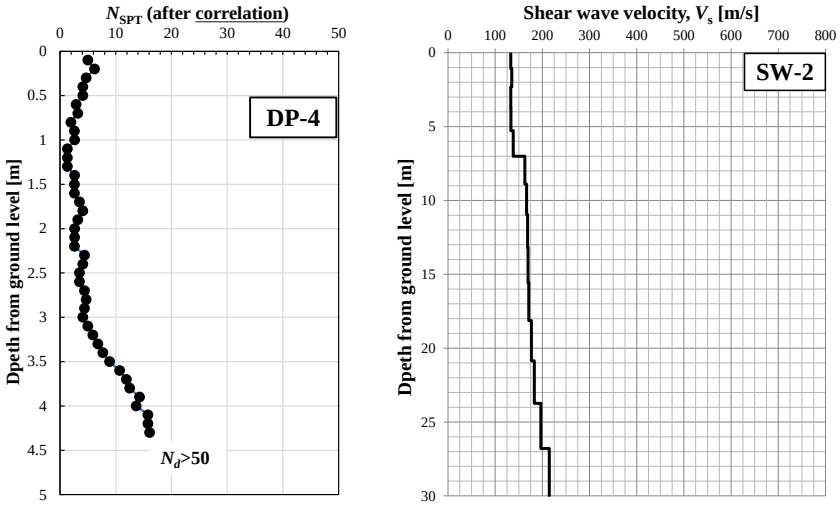

Figure 23. Results of PDCPT at DP-4 and MASW at SW-2

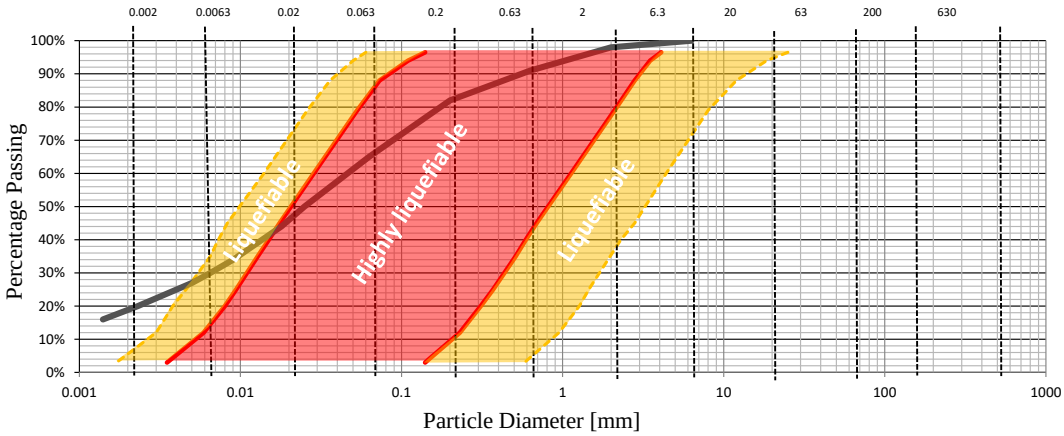

Figure 24. Particle distribution curve of soil ejecta (Sample 3) collected from the town of Golbasi – comparison with critical range associated with liquefaction

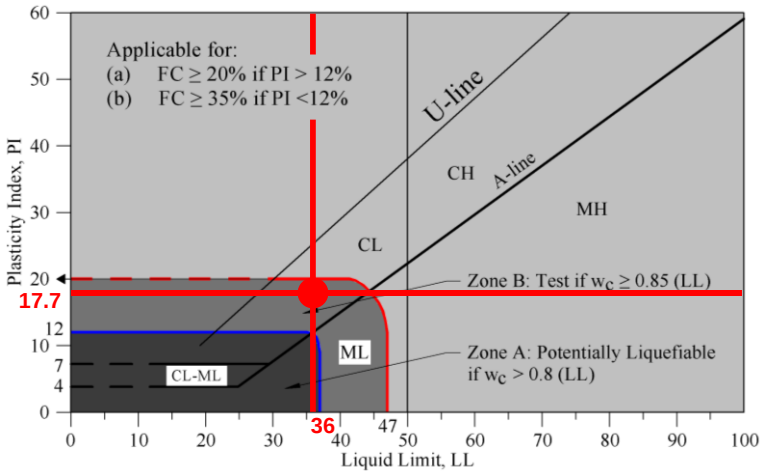

Figure 25. Sample 3 (Golbasi soil ejecta): Liquefaction susceptibility evaluation by adopting the procedure of (Seed et al., 2003)

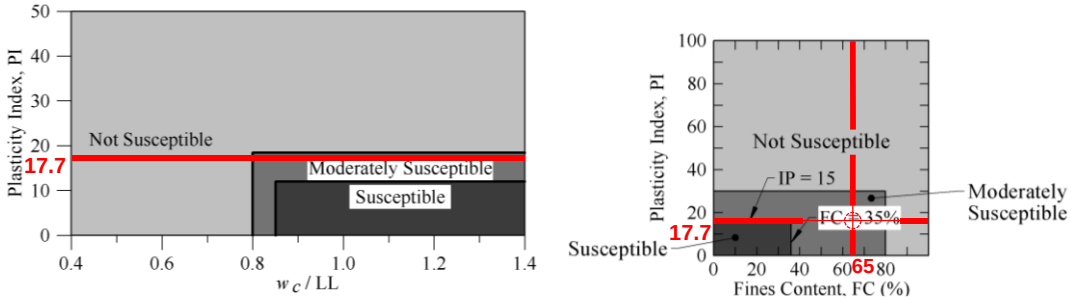

Figure 26. Sample 3 (Golbasi soil ejecta): Liquefaction susceptibility evaluation by adopting the procedure of (Bray & Sancio, 2008), left, and Japanese Road Bridge Design Standards, right

The calculations for the Golbasi site mirrored those for Iskenderun, reaffirming the re-liquefiable nature of the site with a factor of safety (*FS*) consistently below 1.0, following the deterministic approach. This comprehensive assessment encompassed the evaluation of potential liquefaction-induced reconsolidation settlement and lateral spreading (Figure. 27). It is worth emphasizing that the obtained values, while relatively substantial, stem from the limited knowledge of the soil's physical properties. Nonetheless, these cautious estimations emphasize the imperative for more in-depth investigations.

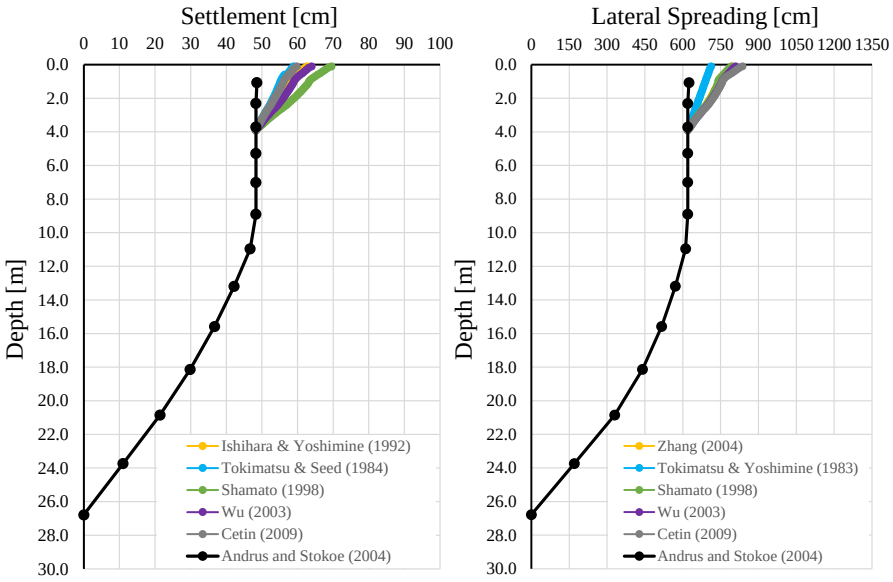

Figure 27. Evaluation of settlement and lateral spreading due to possible re-liquefaction in the town of Golbasi by simplified procedures

The collection of soil samples and the subsequent determination of their physical properties represent a significant step towards a more comprehensive understanding of the geotechnical characteristics in the affected regions. Notably, the determination of a plasticity index (*PI*) within the range of 15 to 20 provides valuable insights into the soil's behavior under seismic loading conditions. Moreover, with direct measurements of average shear wave velocity (V_{s30}) using the multichannel analysis of surface waves (MASW) method and the assumed bulk density (ρ) in the range of 1800 to 2000 kg/m³, it becomes possible to make preliminary estimations of critical parameters. One such parameter is G_{max}, the maximum shear modulus of the soil ejecta, which equals the product of bulk density and shear wave velocity squared, resulting in G_{max} values ranging from 50 to 55 MPa in this context ($G_{max} = \rho \times V_s^2$). Drawing from the work of [24], stiffness degradation curves and damping ratios can be roughly assumed, further enhancing our capacity to model the soil response during seismic events (Figure. 28).

These additional details derived from the physical properties of the soil samples contribute to a more accurate and refined assessment of liquefaction potential and seismic hazard, facilitating the development of robust mitigation strategies for the impacted regions.

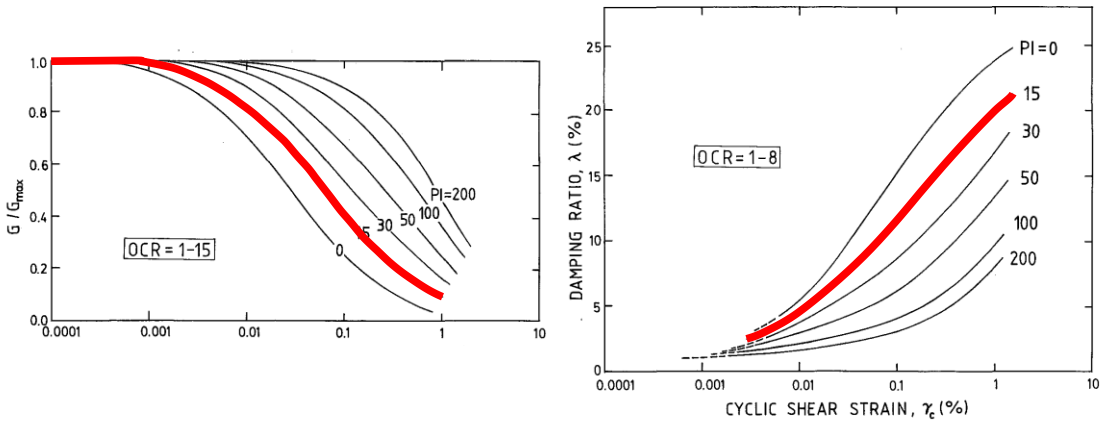

Figure 28. Assumed stiffness degradation and damping ratio in relation with shear strain – tested soil ejecta – after [24]

The stiffness degradation curve and damping ratio play a crucial role in equivalent linear seismic analysis, providing a simplified yet effective approach to model soil behavior during seismic events. By incorporating these parameters into the analysis, it could be understood how the soil responds to varying levels of ground shaking. This, in turn, allows for the estimation of ground motion amplification and the evaluation of structural performance. Equivalent linear analysis is essential because it strikes a balance between accuracy and computational efficiency, making it a valuable tool for seismic hazard assessment and the design of resilient structures. By considering the stiffness degradation curve and damping ratio, engineers and researchers can make informed decisions regarding earthquake-resistant design and mitigate the potential risks associated with liquefaction-induced ground motion.

CONCLUSIONS

In response to the significant seismic events that occurred in Turkey and Syria on February 6th, 2023, a collaborative reconnaissance team was established. This team comprised researchers and engineers from Japan, Turkey, and Bulgaria, representing organizations such as the Japan Association for Earthquake Engineering, the Architectural Institute of Japan, the Japan Society of Civil Engineers, and the Japanese Geotechnical Society, Bogazici University, MEF University, and the University of Architecture, Civil Engineering and Geodesy (UACEG). Their joint efforts led to an extensive on-site investigation conducted from March 28th to April 2nd, 2023, approximately two months after the devastating earthquakes.

During this investigation, several noteworthy findings emerged from various affected areas:

- Iskenderun faced not only building collapses on soft ground but also instances of building tilting and ground subsidence attributed to the liquefaction of reclaimed coastal soil.
- Golbasi witnessed significant damage caused by liquefaction to structures with shallow foundations on soft ground, leading to tilting and settling. However, a more comprehensive investigation is deemed necessary to accurately delineate the extent of liquefied soil layers.

These findings collectively represent the outcome of the collaborative efforts of the reconnaissance team, shedding light on the diverse effects of the earthquakes and the geotechnical challenges faced in the impacted regions.

The initial outcome from the investigations following the seismic events in Turkey and Syria in 2023 highlight the urgent need for further studies in the affected regions. The identification of liquefaction-induced damage in areas like Iskenderun and Golbasi underscores the significance of assessing the re-liquefaction potential. To better comprehend and address the geotechnical challenges posed by these earthquakes, it is crucial to conduct more comprehensive investigations that delve into the specific physical properties of the soil. By obtaining a detailed understanding of the soil's characteristics, it becomes possible to differentiate and potentially exclude certain soil layers from the liquefaction susceptibility analysis. This, in turn, can inform more accurate risk assessments and contribute to the development of resilient engineering solutions for the affected regions. Hence, additional studies hold the key to mitigating future seismic risks and ensuring the safety and stability of infrastructure in earthquake-prone areas.

(Received May 2022, accepted June 2022)

REFERENCES

[1] Damage Control Report by Province. (2023). 023. *KAHRAMANMARAŞ AND HATAY. EARTHQUAKES REPORT. March 2023*. as of March 6th, 2023, https://www.sbb.gov.tr/wp-content/uploads/2023/03/2023-Kahramanmaras-and-Hatay-Earthquakes-Report.pdf,(lastaccessedJune23rd2023)

[2] AFAD-TADAS. (2023). https://tadas.afad.gov.tr/(lastaccessJune10th2023)

[3] Okada, K., Sugiyama, T., Noguchi, T., and Muraishi, H. (1992). A correlation of soil strength between 592 different sounding tests on embankment surface. *Soils and foundations*, 40(4), 11-16..

[4] Toktanis, A., and Over, S. (2021). Konarli Mahallesi'nde (Iskenderun) sivilasma pilot calismasi. 606 *Geosound*, 54(1), 1-11..

[5] DT NEXT. (2023). Roads flooded in Turkey's Iskenderun following quake. *YouTube*, 578 https://www.youtube.com/watch?v=tMl1xzRk6Tw(lastaccessSeptember15th,2023) .

[6] Nalca, C. (2018). Transformation of Iskenderun historic urban fabric from Mid-19th century to the end of 590 the French mandate period. *Master thesis of Izmir Institute of Technology*.

[7] Kramer, S. L. (1996). *Geotechnical earthquake engineering*. Pearson Education India.

[8] Youd, T. L., Idriss, I. M., Andrus, R. D., Arango, I., Castro, G., Christian, J. T., Dobry, E., Finn, W. D. L., Harder Jr., L. F., Hynes, M. E., Ishihara, K., Koester, J. 169 P., Liao, S. S. C., Marcusson III, W. F., Martin, G. R., Mtchell, J. K., Moriwaki, Y., Power, M. S., Robertson, P. K., Seed, R. B., and Stokoe II, K. H. (2001). Liquefaction resistance of soil: Summary report from the 1996 NCEER and 1998 NCEER. In *NSF Workshop on Evaluation of Liquefaction Resistance of Soils" Journal of Geotechnical and Geoenvironmental Engineering*, 124(10), 817-833.

[9] Idriss, I. M., and Boulanger, R. W. (2008). *Soil liquefaction during earthquakes*. Monograph MNO-12, Earthquake Engineering Research Institute, Oakland, CA, 261 pp.

[10] Andrus, R. D., and Stokoe, K. H. (1997). Liquefaction resistance based on shear wave velocity. Proc., *NCEER Workshop on Evaluation of Liquefaction Resistance of Soils, Tech. Rep. NCEER-97-0022*, T. L. Youd and I. M. Idriss, eds., National Center for Earthquake Engineering Research, Buffalo, 89–128.

[11] Cetin, K.O., and R.B. Seed. (2004). Nonlinear shear mass participation factor (r_d) for cyclic shear stress ratio evaluation. *Soil Dynamics and Earthquake Engineering*, 24(2):103–113..

[12] NCEER. (1997). Proceedings of the NCEER Workshop on Evaluation of Liquefaction Resistance of Soils, Edited by Youd, T. L., Idriss, I. M., *Technical Report No. NCEER-97-0022, December 31st, 1997.*

[13] Ishihara, K., and Yoshimine, M. (1992). Evaluation of settlements in sand deposits following liquefaction during earthquakes. *Soils and foundations*, 32(1), 173-188.

[14] Tokimatsu, K., and Seed, H. B. (1984). Simplified procedures of the evaluation of settlements in clean sands. *Rep. No. UCB/GT-84/16*, University of California, Berkeley, California.
[15] Shamoto, Y., Zhang, J., and Tokimatsu, K. (1998). New charts for predicting large residual post-liquefaction ground deformation. *Soil Dynamics and Earthquake Engineering*, 17(7-8), 427-438.
[16] Wu, J., Seed, R. B., and Pestana, J. M. (2003). Liquefaction triggering and post liquefaction deformations of Monterey 0/30 sand under unidirectional cyclic simple shear loading. *Geotechnical Engineering Research Rep. No. UCB/GE 2003/01*, University of California, Berkeley, California.
[17] Cetin, K. O., Bilge, H. T.,Wu, J., Kammerer, A. M., and Seed, R. B. (2009). Probabilistic Model for the Assessment of Cyclically Induced Reconsolidation (Volumetric) Settlements. Journal of Geotechnical Geoenvironmental Engineering, 135(3), 387–398.
[18] Andrus, R. D., Stokoe, K. H., & Hsein Juang, C. (2004). Guide for shear-wave-based liquefaction potential evaluation. *Earthquake Spectra*, 20(2), 285-308.
[19] Zhang, G., Robertson, P. K., & Brachman, R. W. I. (2004). Estimating liquefaction-induced lateral displacements using the standard penetration test or cone penetration test. *Journal of Geotechnical and Geoenvironmental Engineering*, 130(8), 861-871.
[20] Akil, B., Akpinar, K., Uckardesler, C., Araz, H., Saglam, M., Ecemis, B., and Uran, S. B. (2008). Evaluation of Settlement Suitability of Golbasi (Adiyaman) Town, located on the East Anatolian 567 Fault Zone. *Turkiye Jeoloji Bulteni-Geological Bulletin of Turkey*, 51(1), 43-57.
[21] Technical standards for commentaries for port and harbour facilities in Japan. (1999). *Ministry of Transport of Japan* (in Japanese).
[22] Seed, R. B., Cetin, K.O., Moss, R. E. S., Kammerer, A., Wu, J., Pestana, J., Riemer, M., Sancio, R. B., Bray, J. D., Kayen, R. E., & Faris, A. (2003). Recent advances in soil liquefaction engineering: a unified and consistent framework. Keynote presentation, *26th Annual ASCE Los Angeles Geotechnical Spring Seminar*, Long Beach, CA.
[23] Bray, J. D., and Sancio, R. B. (2006). Assessment of the liquefaction susceptibility of fine-grained soils. *Journal of Geotechnical and Geoenvironmental Engineering*. 132 (9): 1165–1177.
[24] Dobry, R., and Vucetic, M. (1987). Dynamic properties and seismic response of soft clay deposits. Proc. *Int. Symp. on Geotech. Engrg. of Soft Soils*, Mexico City, Mexico, 2, 51–87.